



Published in final edited form as:

*Life Sci.* 2021 November 01; 284: 119925. doi:10.1016/j.lfs.2021.119925.

## Development of heart failure with preserved ejection fraction in type 2 diabetic mice is ameliorated by preserving vascular function

Mandy Otto<sup>1</sup>, Laura Brabenec<sup>1</sup>, Melanie Müller<sup>1</sup>, Sebastian Kintrup<sup>1</sup>, Katharina EM Hellenthal<sup>1</sup>, Richard Holtmeier<sup>2</sup>, Sophie Charlotte Steinbuch<sup>1</sup>, Ole Sönken Karsten<sup>1</sup>, Heorhii Pryvalov<sup>1</sup>, Jan Rossaint<sup>1</sup>, Eric R. Gross<sup>3</sup>, Nana-Maria Wagner<sup>1</sup>

<sup>1</sup>Department of Anesthesiology, Intensive Care and Pain Medicine, University Hospital Muenster, Muenster, Germany

<sup>2</sup>Institute of Clinical Radiology, University Hospital Muenster, Muenster, Germany

<sup>3</sup>Department of Anesthesiology, Perioperative and Pain Medicine, Stanford University, Stanford, California, USA

### Abstract

**Aims:** Heart failure with preserved ejection fraction (HFpEF) is associated with endothelial dysfunction and is frequent in people with type 2 diabetes mellitus. In diabetic patients, increased levels of the eicosanoid 12-hydroxyeicosatetraenoic acid (12-HETE) are linked to vascular dysfunction. Here, we aimed to identify the importance of 12-HETE in type 2 diabetic patients exhibiting diastolic dysfunction, and mice exhibiting HFpEF and whether targeting 12-HETE is a means to ameliorate HFpEF progression by improving vascular function in diabetes.

**Material and Methods:** Subjects with diagnosed type 2 diabetes mellitus and reported diastolic dysfunction or healthy controls were recruited and 12(S)-HETE levels determined by ELISA. 12(S)-HETE levels were determined in type 2 diabetic, leptin receptor deficient

---

**Corresponding Author:** PD Dr. med. Nana-Maria Wagner MD, Dept. of Anesthesiology, Intensive Care and Pain Medicine, University Hospital Muenster, Albert-Schweitzer-Campus 1, 48149 Muenster, Germany, Phone: 0049 – 251 83 46837, nmwagner@uni-muenster.de.

**Authors contributions.** MO conducted experiments, acquired and analyzed the data and wrote the manuscript. LB, MM, SK, KEMH, SCC, OSK, HP and JR conducted experiments, acquired, and analyzed the data. ERG provided reagents and revised the manuscript. NMW designed research studies, acquired and analyzed the data and wrote the manuscript.

**Competing interests.** ERG holds a patent on “Peptide modulators of specific calcineurin protein-protein interactions” (US Application Serial No. 16/082,313) that includes the V1-cal peptide. The authors declare that otherwise no competing interests exist.

**Declarations**

**Ethics approval.** The study protocol was approved by the institutional ethics committee of the University Hospital Muenster, Muenster, Germany, and written informed consent was obtained from all study participants. All experimental procedures involving animals were approved by the Animal Care and Use Committees of North Rhine Westphalia, Germany (LANUV).

**Consent for publication.** Not applicable.

**Availability of data and materials.** The datasets generated during and/or analyzed during the current study are available from the corresponding author upon reasonable request. The V1-cal and V1-scr peptides analyzed during the current study are not publicly/commercially available and have been patented by E.R.Gross. It can be made available upon reasonable request.

**Publisher's Disclaimer:** This is a PDF file of an unedited manuscript that has been accepted for publication. As a service to our customers we are providing this early version of the manuscript. The manuscript will undergo copyediting, typesetting, and review of the resulting proof before it is published in its final form. Please note that during the production process errors may be discovered which could affect the content, and all legal disclaimers that apply to the journal pertain.

mice (LepR<sup>db/db</sup>) and HFpEF verified by echocardiography. Mitochondrial function, endothelial function and capillary density were assessed using Seahorse technique, pressure myography and immunohistochemistry in LepR<sup>db/db</sup> or non-diabetic littermate controls. 12/15Lo generation was inhibited using ML351 and 12(S)-HETE action by using the V1-cal peptide.

**Key findings:** Endothelium-dependent vasodilation and mitochondrial functional capacity both improved in response to either application of ML351 or the V1-cal peptide. Correlating to improved vascular function, mice treated with either pharmacological agent exhibited improved diastolic filling and left ventricular relaxation that correlated with increased myocardial capillary density.

**Significance:** Our results suggest that 12-HETE may serve as biomarker indicating endothelial dysfunction and resulting cardiovascular consequences such as HFpEF in type 2 diabetic patients. Antagonizing 12-HETE is a potent means to causally control HFpEF development and progression in type 2 diabetes by preserving vascular function.

### Keywords

Diabetes; heart failure; HFpEF; eicosanoids; endothelial dysfunction; mitochondria

---

### Introduction

Millions of people world-wide suffer from diabetes mellitus and the numbers are increasing. It is estimated that more than half of all patients with diabetes exhibit poorly controlled glucose and ~30% uncontrolled arterial hypertension and these numbers remained unchanged during the past decade [1]. Hyperglycemia, arterial hypertension and the chronic low-grade inflammatory condition associated with type 2 diabetes mellitus almost inevitably and mostly already shortly after disease onset lead to endothelial dysfunction and microvascular disease that contributes to cardiovascular disease development and progression in patients with diabetes. In particular, it is estimated that ~50% of patients with diabetes have heart failure with preserved ejection fraction (HFpEF) [2]. HFpEF is characterized by diastolic dysfunction with abnormal left ventricular filling and elevated filling pressures but unlike as in heart failure with reduced ejection fraction (HFrEF), a preserved left ventricular ejection fraction (LVEF) [3]. In diabetic patients, HFpEF is believed to primarily develop based on the impairment of the left ventricular microvasculature from hyperglycemia, hypertension and inflammation that results ventricular stiffening [4]. Importantly, patients with HFpEF exhibit similarly high morbidity and mortality as patients with HFrEF [5], but effective treatment options have not been identified. This is mainly attributable to the substantially different pathophysiology of HFpEF in contrast to HFrEF, resulting in an absence of benefit of patients with HFpEF from guideline-based heart failure medication [6]. In turn, therapeutic strategies that can preserve vascular function despite the ongoing diabetic condition may display promising approaches to ameliorate HFpEF progression and improve the outcomes for millions of patients worldwide [4].

At the cellular level, the uncontrolled plasma glucose levels and a systemic low-grade inflammatory condition trigger oxidative stress in the myocardial vasculature that exceeds

the buffering capacity of the mitochondria [4]. Patients with diabetes exhibit damaged endothelial mitochondria with mitochondrial calcium overload that increases the level of reactive oxygen species, reduces the bioavailability of endothelial nitric oxide and results in impaired endothelium-driven vasodilation [7, 8]. Endothelial dysfunction is common among patients with HFpEF and an impaired myocardial microvascular function facilitates the development of fibrotic myocardial reorganization, leading to ventricular stiffening and impaired ventricular relaxation [4]. Mechanistically, uncontrolled plasma glucose induces an increased break down of arachidonic acid by 12-lipoxygenase (12LOX, 12/15LO in mice) to 12(S)-hydroperoxyeicosatetraenoic acid (12(S)-HETE) [9]. We have previously reported evidence that endothelial cells are a major contributor to elevated 12(S)-HETE levels under hyperglycemic conditions and that elevated 12(S)-HETE levels can be found increased in the plasma of type 1 diabetic patients and also type 2 diabetic patients with coronary artery disease [10–12]. While the role of 12(S)-HETE in compromising mitochondrial function in the diabetic endothelium had long been described [13], we have recently unraveled the mechanisms that link elevated 12(S)-HETE levels in the endothelium to mitochondrial calcium overload and endothelial dysfunction in type 1 diabetic mice [10].

Here, we report that type 2 diabetic patients with diastolic dysfunction have elevated 12(S)-HETE levels and identify that targeting endothelial 12(S)-HETE generation or action can preserve vascular integrity and augment diastolic function in an established mouse model of diabetes-induced HFpEF [14–16].

## Research Design and Methods.

### Study design and population:

The study protocol was approved by the institutional ethics committee of the University Hospital Muenster, Muenster, Germany, and written informed consent was obtained from all study participants. Male and female patients with and without type 2 diabetes (HbA1c <6% vs. HbA1c >7%, respectively) were recruited and peripheral venous blood was collected using sodium-heparin as anticoagulant and stored at –80°C upon analysis. Parameters such as age, gender, primary disease, arterial hypertension, medication, fasted blood glucose levels, HbA1c listed in Table 1 were obtained. In addition, previous echocardiographic evaluations were screened for the reports of diastolic dysfunction.

### Animals.

All experimental procedures were approved by the Animal Care and Use Committees of North Rhine Westphalia, Germany (LANUV). Heterozygous B6.BKS(D)-Leprdb/J (LepR<sup>db/+</sup>) mice were obtained from the Jackson laboratory and bred with ad libitum access to food and water. Heterozygous B6.BKS(D)-Leprdb/J (LepR<sup>db/+</sup>) and homozygous wild type B6.BKS(D)-Leprdb/J (LepR<sup>+/+</sup>) served as non-diabetic control mice to homozygous, obese and diabetic B6.BKS(D)-Leprdb/J (LepR<sup>db/db</sup>). Genotypes were confirmed via PCR and gel electrophoresis using the following primers as previously published [17]: forward outer primer 5'TTGTTCCCTTGTTCTTATACCTATTCTGA-3', reverse outer primer 5'CTGTAACAAAATAGGTTCTGACAGCAAC-3', forward inner primer 5'ATTAGAAGATGTTTACATTTTGATGGAAGG-3', reverse inner primer

5'GTCATTCAAACCATAGTTTGGTTTGTCTA-3'. Diabetes onset was confirmed by measurement of non-fasted blood glucose levels using an Accu-Check Performa glucometer (Roche, Basel, Switzerland). Diabetic mice had increased body weight and blood glucose levels at 12 weeks of age. Blood plasma samples were obtained from the facial vein. 12(S)-HETE and 15(S)-HETE levels were assessed using enzyme-linked immunosorbent assays (Enzo LifeSciences, Lörrach, Germany). 12/15Lo-CdH5Cre mice were used for generating a tamoxifen-inducible, endothelium-specific 12/15lipoyxygenase knock out (endothelium-specific 12/15Lo knockout mice) as described before [10].

### Small molecule and peptide application.

Diabetic LepR<sup>db/db</sup> mice were treated with 5-(Methylamino)-2-(1-naphthalenyl)-4-oxazolecarbonitrile (ML351, 100mg/kg intraperitoneally for seven days, Tocris, Bristol, UK), a highly specific inhibitor for human and murine 12LOX and 12/15LO, respectively [18]. To block 12-HETE action, mice were treated with the peptide RAITILDTEKS linked to a TAT-linker for intracellular entry (V1-cal, 1mg/kg/d intravenously for 4 days) or scrambled peptide IDKLRTAEIST (V1-scr, 1mg/kg/d intravenous for 4 days) [10, 19].

### Pressure Myography.

To assess endothelial function, third order mesenteric resistance arteries were dissected and mounted on glass cannulas in a vessel chamber (Living Systems Instrumentation). Chamber and tubing were filled with calcium containing buffer (10mM HEPES, 140mM NaCl, 5mM KCl, 1.2mM MgCl<sub>2</sub>, 10mM Glucose, 2mM CaCl<sub>2</sub>). After the development of stable myogenic tone at 80mmHg, vessels were exposed to 10nM (R)-(-)-phenylephrine hydrochloride (Phe) for maximum constriction. Relaxation response to increasing concentrations of carbamoylcholine chloride (Cch, 10<sup>-9</sup> to 10<sup>-5</sup>M) was constantly recorded using digital video edge-detection. A subset of vessels was exposed to 100µM N(ω)-nitro-L-arginine methyl ester (L-NAME) to verify Cch-effects depend on endothelium-dependent nitric oxide release or to 1µM 12(S)-HpETE for 15min before Phe administration.

### Isolation of murine endothelial cells.

Murine pulmonary microvascular endothelial cells were isolated from mice using magnetic sheep anti-rat IgG-coated Dynabeads® (Invitrogen, Carlsbad, USA, Cat.-No. 11035) coated with rat anti-mouse CD31 antibody (MEC13.3, Biolegend, San Diego USA) as previously published [10]. In brief, mice were sacrificed by cervical dislocation and the lungs were flushed with PBS, minced and incubated in collagenase solution (20mg collagenase, 25µL 1M CaCl<sub>2</sub>, 200µL PenStrep, 10µL DNase, ad 20mL PBS) to obtain single cell solutions. Following filtration through a 70µm cell strainer, cell solutions were centrifuged 10 min at 0.4 rcf. Pellets were resuspended in 2mL washing medium (DMEM, 10% FCS, 1% PenStrep) and incubated with CD31-coupled anti-rat IgG-coated Dynabeads® on a rotator for 45min at 4°C. Tubes were placed in a magnetic separator to separate bead-coupled cells that were directly used to assess mitochondrial function using a Seahorse flux analyzer.

### Mitochondrial function.

Ex vivo mitochondrial function of murine endothelial cells was investigated using an XFp Seahorse extracellular flux analyzer (Agilent, Santa Clara, USA). 30,000 cells were seeded in Seahorse Miniplates in Seahorse XF DMEM medium (103575–100, Agilent, Santa Clara, USA) supplemented with 1% FCS, 2mM L-glutamine, 1mM pyruvate and 5.5mM D-glucose, adjusted to pH 7.4 using 1M NaOH directly after isolation. In some experiments, cells were exposed to 1 $\mu$ M baicalein (Tocris, Bristol, UK), 100nM BCTC (Tocris, Bristol, UK) or DMSO as vehicle control for 2h prior analysis. In other experiments, endothelial cells of in vivo treated mice were used. Miniplates were centrifuged for 20min at 2000g at room temperature. All experiments were performed using the Mito Stress Test Kit (Agilent, Santa Clara, USA, 103010–100) containing oligomycin, FCCP and antimycin/rotenone.

### Immunohistochemistry.

Murine hearts were embedded in optimal cutting temperature compound the day of sacrifice, frozen and stored at  $-80^{\circ}\text{C}$ . For immunohistochemistry 7 $\mu\text{m}$  cryosections were fixed for 10min in precooled acetone at  $-20^{\circ}\text{C}$  and blocked using 5% BSA/PBS for 30min at room temperature: anti-CD31 primary antibody (Purified Rat Anti-Mouse CD31, Clone MEC 13.3, 550274, Bioscience, Heidelberg, Germany) was diluted 1:200 in blocking solution and incubated over night at  $4^{\circ}\text{C}$  before incubation for 1h at room temperature with donkey anti-rat secondary antibody (Donkey anti-Rat IgG (H+L) Highly Cross-Adsorbed Secondary Antibody, Alexa Fluor 488, A-21208, Thermo Fisher, Waltham, USA). Nuclear staining was performed using 2.5 $\mu\text{g}/\text{ml}$  4',6-Diamidin-2-phenylindol (DAPI) in PBS for 5min at room temperature. Slides covered using fluorescence mounting medium and imaged with LSM700 laser confocal microscope using 40-fold magnification.

### Echocardiography:

For ultrasound examinations 12–14 week old mice were anesthetized using isoflurane (4–5% in 1L O<sub>2</sub>/min). Anesthesia was maintained with 2.0% isoflurane. The animals were depilated ventrally and heart rate, breathing and body temperature were monitored throughout the experiment. An ultrasound probe (Vevo 2100 by VisualSonics with 18–55 MHz transducers MS400 and MS550D) was used to assess left ventricular ejection fraction calculated using Simpson's method. From the pulse wave Doppler curve,  $E_{\text{max}}$  and  $A_{\text{max}}$  and consequently, E/A were determined. Tissue doppler imaging (TDI) was used to analyze the velocity of the medial or lateral mitral annulus.  $E'$  and  $A'$  were then extracted from TDI curve and ratios calculated. All parameters were analyzed by using Vevo Lab 2.2.0 software.

### Western blot.

Fat tissue lysates of non-diabetic, diabetic and ML351 or V1-cal treated LepR<sup>db</sup> mice were resolved by SDS-PAGE and transferred to a PVDF membrane. Proteins were detected by anti-TRPV1 (ACC-030, Alomone Labs) and anti-actin (MA5–15739, Thermo Fischer Scientific). For visualization, developing kits for horseradish peroxidase–conjugated secondary antibodies were used.

## Statistical analysis.

Statistical analysis was performed using Graph Pad Prism 7 software (GraphPad Software Inc.). A Shapiro-Wilk normality test was performed to test for normal distribution and Students t-test or Mann-Whitney U-test used for the comparison of two groups. For the comparison of three or more groups, a One-way ANOVA followed by Bonferroni correction for multiple comparisons or the Kruskal-Wallis test was performed. For repeated comparisons of multiple groups over time, a Two-way ANOVA followed by Bonferroni correction was used. For comparison of categorical parameters, the McNemar test was used, correlation was assessed using Pearson's correlation. A P-value <0.05 was considered statistically significant. Data is presented as mean±SEM.

## Results

### Reduction of high levels of 12(S)-HETE in diabetes improves vascular function and ameliorates HFpEF.

To first determine the relevance of 12(S)-HETE in the pathophysiology of human HFpEF, we recruited diabetic patients with previously reported diastolic dysfunction characteristics. Compared to non-diabetic controls, diabetic patients exhibiting diastolic dysfunction had elevated levels of fasting blood glucose (139±39 mg/dL), increased HbA1c values (7.2±0.9%) and increased levels of 12(S)-HETE (264.2±93.2 vs. 17.6±2.8ng/mL in non-diabetic controls, n=13 patients/group, P=0.014, Table 1, Figure 1A). Of note, 12(S)-HETE levels showed a tight correlation with HbA1c values (P=0.017). In contrast to 12(S)-HETE, 15(S)-HETE levels were low and not elevated in type 2 diabetic patients (14.3±3.6 vs. 6.7±0.7ng/mL in non-diabetic controls, Figure 1A). We then used a mouse model of type 2 diabetes mellitus and confirmed elevated levels of 12(S)-HETE in these mice at 12 weeks of age and manifest diabetes (642.4±130.7 in type 2 diabetic vs. 268.4±56.6ng/mL in non-diabetic controls, P<0.01, n=13–14 mice/group, Figure 1B). In contrast and comparable to humans, 15(S)-HETE levels were not elevated (32.9±3.1ng/mL in non-diabetic and 45.6±5.5ng/mL in diabetic mice). We next used the small molecule 12/15LO inhibitor ML351 to reduce endogenous 12(S)-HETE production (from 642.4±130.7 to 112.3±17.3ng/mL, P<0.001, n=10 ML351 treated mice, Figure 1C) and confirmed reduced 12(S)-HETE levels can improve endothelium-dependent vasodilation in diabetic mice (improvement from 80.4±4.3% remaining phenylephrine-induced vasoconstriction to only 51.1±11.9% in ML351-treated, diabetic mice in response to carbamoylcholine stimulation, P<0.001 vs. diabetic, control-treated mice, n=8–12 mice/group, Figure 1D, E). Of note, exogenously administered 12(S)-HpETE, simulating high 12(S)-HETE levels of diabetic mice, reduced the endothelium dependent vasodilation in otherwise healthy wild type mice (Suppl. Figure 1).

To assess whether improved endothelial function is associated with improved characteristics of diastolic dysfunction and HFpEF characteristics, we conducted echocardiography in diabetic mice and diabetic mice subjected to ML351 treatment as well as wet-to-dry lung weight and heart weight to tibia length ratio. As reported previously, the heart weight to tibia length was not affected by type 2 diabetes in leptin receptor deficient mice (Suppl. Figure 5, Suppl. Table 1) [20]. Application of the 12LOX inhibitor ML351 augmented diastolic



function of diabetic mice (decrease of E/A ratio from  $1.87 \pm 0.1$  to  $1.49 \pm 0.04$ ,  $P < 0.001$ ,  $n = 8-11$  mice/group and decrease of E/E' ratio from  $59.61 \pm 6.24$  to  $40.4 \pm 4.47$ ,  $P < 0.01$ ,  $n = 8-10$  mice/group) to the level of non-diabetic controls (Figure 1H–J). Importantly, improvement of diastolic left ventricular function in diabetic mice was associated with a restoration of capillary density compared to untreated diabetic mice that exhibited left ventricular muscle tissue capillary rarefaction (from  $329.7 \pm 52.23$  in diabetic to  $632.1 \pm 57$  capillaries/ $\text{mm}^2$  in diabetic, ML351-treated mice,  $P < 0.01$ ,  $n = 5$  mice/group, Figure 1K, L). The inhibition of 12LOX or endothelial knock out of 12/15LO had no effect on left ventricular capillary density (Figure 1K, L, Suppl. Figure 2). These data confirmed sufficient 12/15LO inhibition that results in reduced 12(S)-HETE plasma levels despite ongoing diabetes can improve endothelial function that is associated with ameliorated HFpEF characteristics.

### **Reduction of 12(S)-HETE generation or action protects mitochondrial function in type 2 diabetes mellitus.**

At the mechanistic level, 12(S)-HETE-induced endothelial dysfunction is mediated by an impaired mitochondrial function from mitochondrial calcium overload [10]. Endothelial cells from type 2 diabetic mice showed impaired mitochondrial respiration that was augmented by 12/15LO inhibition in vitro using baicalein (increase from  $0.6 \pm 0.04$  to  $1.2 \pm 0.06$ -fold mitochondrial reserve capacity,  $P < 0.001$ ,  $n = 5-6$  mice/group Figure 2A–C, Suppl. Figure 3A, B). We confirmed the role of an improved mitochondrial function also in endothelial cells isolated from diabetic mice treated in vivo with ML351 that then exhibited improved mitochondrial functional characteristics (from  $0.7 \pm 0.05$  in diabetic mice back to the baseline  $1.0 \pm 0.1$ -fold of non-diabetic controls,  $P < 0.05$ , endothelial cells from  $n = 5-8$  mice/group, Figure 2D–F, Suppl. Figure 3C, D). 12(S)-HETE adverse effects at the mitochondria are mediated by activation of the mitochondrial calcium channel transient receptor potential vanilloid 1 (TRPV1) that then triggers mitochondrial calcium overload [10]. In vitro, mitochondrial functional characteristics in isolated endothelial cells were improved by inhibition of TRPV1 (from  $0.6 \pm 0.05$ -fold mitochondrial reserve capacity in endothelial cells from diabetic mice to  $1.1 \pm 0.2$ -fold mitochondrial reserve capacity in endothelial cells from diabetic mice treated in vitro with the TRPV1 inhibitor BCTC,  $P < 0.05$ , endothelial cells from  $n = 6$  mice/group, Figure 2G–J, Suppl. Figure 3E, F). Finally, we used a peptide, V1-cal, that mimics a TRPV1 TRP box motif serving as binding site of 12(S)-HETE as a decoy to prevent 12(S)-HETE induced TRPV1 activation at the mitochondria [10]. Of note, TRPV1 expression was not affected under hyperglycemic condition or after pharmaceutical treatments (Suppl. Figure 4). Intravenous application of this peptide to diabetic mice improved mitochondrial function in endothelial cells isolated from diabetic mice (from  $0.8 \pm 0.06$ -fold in diabetic mice treated with a scrambled version of the V1-cal peptide, V1-scr, to  $1.1 \pm 0.06$ -fold in diabetic, V1-cal-treated mice,  $P < 0.01$ , endothelial cells from  $n = 6$  mice/group, Figure 2K–M, Suppl. Figure 3G, H). Taken together, we here confirmed that inhibition of 12(S)-HETE inhibition or action are both potent means to ameliorate diabetes-induced mitochondrial dysfunction.

## Abrogation of 12(S)-HETE-induced TRPV1 activation restores endothelial function and diastolic ventricular relaxation in type 2 diabetic mice.

As a consequence of an improved endothelial cell mitochondrial function in diabetic mice, V1-cal-treated type 2 diabetic mice exhibited almost restored endothelium-dependent vasodilation (from  $80.3 \pm 1.2\%$  remaining vasoconstriction in diabetic, V1-scr treated mice to  $38.5 \pm 9.2\%$  vasoconstriction in V1-cal-treated mice,  $P < 0.001$ ,  $n = 7-12$  mice/group, Figure 3A, B). In line with improved endothelial function, application of the V1-cal peptide preventing 12(S)-HETE/TRPV1 interaction, but not of V1-scr, prevented HFpEF development in type 2 diabetic LepR<sup>db/db</sup> mice: Use of the peptide resulted in normalized early-to-late stage (E/A) diastolic filling rates compared to diabetic mice and diabetic, V1-scr-treated mice ( $1.57 \pm 0.04$  in V1-cal-treated mice vs.  $1.90 \pm 0.01$  in diabetic mice,  $P < 0.05$ ,  $n = 7-9$  mice/group and vs.  $2.0 \pm 0.4$  in V1-scr-treated mice,  $P < 0.01$ ,  $n = 5$  mice/group) and mitral wave E to E' ratios ( $43.6 \pm 5.44$  in V1-cal-treated mice vs.  $65.3 \pm 5.55$  in diabetic mice,  $P < 0.05$ ,  $n = 9-10$  mice/group Figure 3 C–F). To note, neither V1-cal nor ML351 affected lung weight or heart weight-to-tibia ratio in diabetic mice (Suppl. Figure 5, Suppl. Table 1). Comparable to 12/15LO inhibition, V1-cal application was associated with augmented capillary density in left ventricles of type 2 diabetic mice ( $900 \pm 222$  in V1-cal-treated vs.  $468.5 \pm 25.7$  capillaries/mm<sup>2</sup> in V1-scr-treated mice,  $P < 0.05$ ,  $n = 5$  mice/group, Figure 3G, H). This data supports the importance of mitochondrial TRPV1 as the downstream effector of increased endothelial 12(S)-HETE levels in diabetes and highlights the inhibition of 12(S)-HETE action as a second therapeutic strategy effective in improving vascular and left ventricular diastolic function.

## Discussion

In this study we characterize 12(S)-HETE plasma concentration is elevated in type 2 diabetic humans and mice both exhibiting diastolic dysfunction that is characteristic of heart failure with preserved ejection fraction (HFpEF). Inhibiting the generation or action of these increased 12(S)-HETE levels in type 2 diabetic mice restored mitochondrial function in the endothelium and was associated with improved endothelium-dependent vasodilation and augmented left ventricular-capillary density. These findings together correlated with improved left ventricular diastolic filling patterns despite ongoing diabetes, suggesting that we have identified 12(S)-HETE as a potent target to treat HFpEF by augmenting vascular function in type 2 diabetes mellitus.

Roughly 1% of the Western world suffers from HFpEF [21]. Like no other disease affecting this large number of patients in the 21<sup>st</sup> century, HFpEF is left almost untreated, as no specific therapeutics are available [22]. In contrast to HFrEF, where clinical comorbidities such as obesity or diabetes are *associated* with the disease, the current notion is that HFpEF is rather *caused* by these comorbidities [23]. Both obesity and diabetes lead to elevation of glucose levels in the blood that – already in healthy individuals one hour after ingestion of a sugar-loaded soft-drink – impair endothelium-driven vasoreactivity [24]. The ability of the endothelium to mediate relaxation of the smooth muscle cells in the tunica media of the vessel wall is primarily mediated by nitric oxide (NO), with reduced NO bioavailability making up the hallmark of both obesity and diabetes-induced first-entity vascular endothelial



dysfunction. In patients with HFpEF, reduced coronary blood flow reserve is detected, most likely derived from a reduction of NO liberation by coronary endothelial cells [25]. In this regard, reducing the availability of NO was primarily used recently to establish a mouse model of HFpEF [26] that exhibits comparable HFpEF characteristics as the LepR<sup>db/db</sup> mouse model used in this study [14] and drugs that target the nitrate-nitrite-NO pathway are currently discussed as the most promising drugs for a potential treatment of HFpEF [27].

In the pathogenesis of diabetes and obesity-induced reduction of NO bioavailability and the resulting endothelial dysfunction, impairment in endothelial calcium handling plays a key role in disturbing endothelial homeostasis. Transient receptor potential (TRP) channels are involved in endothelial calcium handling and extensive evidence points towards a key role of this receptor superfamily for both obesity and diabetes-induced vascular dysfunction [28]. We have recently identified the TRP vanilloid 1 (TRPV1) subtype as located intracellularly, mainly at endothelial mitochondria, and dissected its importance in mediating mitochondrial calcium overload in type 1 diabetes [10]. Importantly, we identified the primary endogenous activator of TRPV1, 12(S)-HETE, that is the most potent lipid peroxidation product to activate TRPV1 [29] and the only lipid peroxidation product specifically found increased in type 1 diabetic rats (E.R. Gross, unpublished observation), type 1 diabetic mice [10] and humans [11]. Moreover, despite platelet-derived 12(S)-HETE, endothelial cells are a major contributor to the increased 12(S)-HETE plasma concentrations in diabetic mice and patients [10]. Here, we confirm 12(S)-HETE levels are elevated in type 2 diabetic mice and humans. Of note, the 12(S)-HETE levels in diabetic patients were clearly above the 350nM (~117ng/mL) threshold that is the  $K_I$  of 12(S)-HETE to activate calcium flux via TRPV1 [29]. Increased lipid peroxidation driven by the 12/15LO/12(S)-HETE system has previously been implicated in the pathogenesis of vascular dysfunction and atherosclerosis progression. In turn, drugs targeting 12/15LO activity are discussed as promising therapeutics to tackle vascular dysfunction specifically in diabetes mellitus [13]. Interestingly, other therapeutical approaches that are currently under development for treatment of HFpEF are also associated with mitigating endothelial lipid peroxidation. For example, sodium-glucose-transporter-2 inhibitors improve HFpEF in diabetic patients and rats by reducing endothelial lipid peroxidation [30]. We here dissect in detail the direct effects of a reduced 12(S)-HETE production or action on augmenting endothelium-driven vasodilation and show that this augmentation of vascular function directly affects the detection of typical characteristics of HFpEF that we otherwise found developed in type 2 diabetic mice already four weeks after – which is by definition – type 2 diabetes onset. In contrast, previous studies could detect HFpEF only in older mice between 4.5 to 6 months of age [14, 15, 31], and the potential intervention strategies against cardiac dysfunction were performed over long periods like 28 days [31, 32] or were reported as unsuccessful after all [15]. In this regard, early detection and targeting of HFpEF may have allowed us to conduct a successful treatment of diastolic dysfunction in type 2 diabetic mice. This may point towards the importance of early and preventative strategies against diabetes-associated comorbidities such as HFpEF, as they may remain irreversible during later stages of diabetes-induced vascular dysfunction. Future studies will have to determine the windows of opportunity for preventing HFpEF most likely based on a preserved plasticity of the cardiac microvascular bed.

In addition to targeting the 12/15LO/12(S)-HETE system by inhibiting 12/15LO, we here also inhibited the downstream action of 12(S)-HETE on the TRPV1 channel and the inhibition of TRPV1 itself using specific inhibitors. TRPV1 is a nociceptor also located in the cardiac and vascular system where it primarily gates calcium [33]. Interestingly and extending our previous report to the heart, the cardioprotective effects of 12/15LO inhibition, for example by baicalein, on heart failure, were previously related to the modulation of calcium handling [34]. The V1-cal peptide described previously [19] mimics the putative TRPV1 binding site of 12(S)-HETE located in the C-terminal TRP-box of TRPV1 serving as a decoy for 12(S)-HETE [10]. In mice treated with the V1-cal peptide, 12(S)-HETE plasma levels cannot be detected, most likely as the 12(S)-HETE-V1-cal complex is undetectable to the corresponding analysis. Thus, the peptide allows to selectively abrogate TRPV1 activation in high 12(S)-HETE conditions, thus reducing mitochondrial calcium overload. Recently, TRPV1 has also been implicated in modulating immune responses by being expressed on sensory nerve ending in the bone marrow [35]. Both obesity and diabetes are associated with a chronically low-grade inflammation that at least in part causes disruption of the tight regulation of vascular tone and the microvascular milieu within the heart. In HFpEF in particular, increased numbers of inflammatory cells are recruited to the myocardium that then drive ventricular stiffening by promoting fibrosis [3, 36]. Thus, it may be suggested that modulating TRPV1 is a means to modulate the inflammatory response that otherwise drives HFpEF development and progression in obesity and diabetes.

## Limitations

A limitation of the present study is the small cohort of diabetic patients, in whom elevated 12(S)-HETE levels were measured, that does not represent the global collective of type 2 diabetic patients. The study participants recruited had reported findings of diastolic dysfunction based on echocardiographic findings, but additional parameters required for the diagnosis of HFpEF (i.e. clinical symptoms as well as levels of N-terminal B-type natriuretic peptides (NTproBNP)) were not determined. In addition, HFpEF is a complex, multifactorial disease and although leptin-receptor deficient mice are an established preclinical model resembling the main HFpEF characteristics, the model does not suffice to represent all facets of HFpEF in human patients. Further, this study does not elaborate the contribution of smooth muscle cell dysfunction to the diabetes-induced vascular pathology or possible side effects of ML351 or V1-cal injections like compensatory effects through other pathways.

## Conclusion

Taken together, we provide evidence that HFpEF development can be prevented or at least delayed during early stages of type 2 diabetes by specifically targeting the endothelial mechanism driving impaired endothelium-dependent vasodilation in type 2 diabetic mice. Future studies are needed to identify whether the protection of left ventricular function in diabetes mellitus can be added to the promising portfolio of small molecule 12LOX inhibitors due to their ability to preserve endothelial functional properties in the diabetic cardiac microvasculature.

## Supplementary Material

Refer to Web version on PubMed Central for supplementary material.

## Acknowledgements.

The authors thank Christiane Geyer from the European Institute for Molecular Imaging (EIMI) at the Medical Faculty of the University of Muenster for technical support in conducting echocardiography in diabetic mice.

## Funding.

This work was funded by funded by NIGMS GM119522 (ERG) and the Deutsche Forschungsgemeinschaft (German Research Foundation) to NMW (WA3786/3-1 and WA3786/2-1).

## References

1. Fang M Trends in diabetes management among US adults: 1999–2018. *N. Engl. J. Med.* 2021;384(23):2219–28. [PubMed: 34107181]
2. Bouthoorn S, Valstar GB, Gohar A, et al. The prevalence of left ventricular diastolic dysfunction and heart failure with preserved ejection fraction in men and women with type 2 diabetes: A systematic review and meta-analysis. *Diabetes and Vascular Disease Research.* 2018;15(6):477–93. [PubMed: 30037278]
3. Paulus WJ, Tschöpe C, Sanderson JE, et al. How to diagnose diastolic heart failure: a consensus statement on the diagnosis of heart failure with normal left ventricular ejection fraction by the Heart Failure and Echocardiography Associations of the European Society of Cardiology. *Eur. Heart J.* 2007;28(20):2539–50. [PubMed: 17428822]
4. D'Amario D, Migliaro S, Borovac JA, et al. Microvascular dysfunction in heart failure with preserved ejection fraction. *Front. Physiol.* 2019;10:1347. [PubMed: 31749710]
5. Owan TE, Hodge DO, Herges RM, Jacobsen SJ, Roger VL, Redfield MM. Trends in prevalence and outcome of heart failure with preserved ejection fraction. *N. Engl. J. Med.* 2006;355(3):251–9. [PubMed: 16855265]
6. Borlaug BA, Paulus WJ. Heart failure with preserved ejection fraction: pathophysiology, diagnosis, and treatment. *Eur. Heart J.* 2011;32(6):670–9. [PubMed: 21138935]
7. Shenouda SM, Widlansky ME, Chen K, et al. Altered Mitochondrial Dynamics Contributes to Endothelial Dysfunction in Diabetes Mellitus Clinical Perspective. *Circulation.* 2011;124(4):444–53. [PubMed: 21747057]
8. Lowell BB, Shulman GI. Mitochondrial dysfunction and type 2 diabetes. *Science.* 2005;307(5708):384–7. [PubMed: 15662004]
9. Patricia MK, Natarajan R, Dooley AN, et al. Adenoviral delivery of a leukocyte-type 12 lipoxygenase ribozyme inhibits effects of glucose and platelet-derived growth factor in vascular endothelial and smooth muscle cells. *Circ. Res.* 2001;88(7):659–65. [PubMed: 11304487]
10. Otto M, Bucher C, Liu W, et al. 12 (S)-HETE mediates diabetes induced endothelial dysfunction by activating intracellular endothelial cell TRPV1. *The Journal of Clinical Investigation.* 2020.
11. Hennessy E, Rakovac Tisdall A, Murphy N, et al. Elevated 12-hydroxyeicosatetraenoic acid (12-HETE) levels in serum of individuals with newly diagnosed Type 1 diabetes. *Diabet. Med.* 2016.
12. Zhang HJ, Sun CH, Kuang HY, et al. 12S-hydroxyeicosatetraenoic acid levels link to coronary artery disease in Type 2 diabetic patients. *J. Endocrinol. Invest.* 2013;36(6):385–9. doi:10.3275/8654 [PubMed: 23095287]
13. Dobrian A, Morris M, Taylor-Fishwick D, et al. Role of the 12-lipoxygenase pathway in diabetes pathogenesis and complications. *Pharmacol. Ther.* 2019;195:100–10. [PubMed: 30347209]
14. Alex L, Russo I, Holoborodko V, Frangogiannis NG. Characterization of a mouse model of obesity-related fibrotic cardiomyopathy that recapitulates features of human heart failure with preserved ejection fraction. *American Journal of Physiology-Heart and Circulatory Physiology.* 2018;315(4):H934–H49. [PubMed: 30004258]

15. Methawasin M, Strom J, Borkowski T, et al. Phosphodiesterase 9a inhibition in mouse models of diastolic dysfunction. *Circ. Heart Fail.* 2020;13(5):e006609. [PubMed: 32418479]
16. Valero-Muñoz M, Backman W, Sam F. Murine models of heart failure with preserved ejection fraction: a “fishing expedition”. *Basic to Translational Science.* 2017;2(6):770–89. [PubMed: 29333506]
17. Peng B-y, Wang Q, Luo Y-h, He J-f, Tan T, Zhu H. A novel and quick PCR-based method to genotype mice with a leptin receptor mutation (db/db mice). *Acta Pharmacol. Sin.* 2018;39(1):117–23. [PubMed: 28748911]
18. Rai G, Joshi N, Perry S, et al. Discovery of ML351, a potent and selective inhibitor of human 15-lipoxygenase-1. *Probe Reports from the NIH Molecular Libraries Program [Internet].* 2014.
19. Hurt CM, Lu Y, Stary CM, et al. Transient Receptor Potential Vanilloid 1 Regulates Mitochondrial Membrane Potential and Myocardial Reperfusion Injury. *Journal of the American Heart Association.* 2016;5(9):e003774. [PubMed: 27671317]
20. Reil J-C, Hohl M, Reil G-H, et al. Heart rate reduction by I f-inhibition improves vascular stiffness and left ventricular systolic and diastolic function in a mouse model of heart failure with preserved ejection fraction. *Eur. Heart J.* 2013;34(36):2839–49. [PubMed: 22833515]
21. Lam CS, Donal E, Kraigher-Krainer E, Vasan RS. Epidemiology and clinical course of heart failure with preserved ejection fraction. *Eur. J. Heart Fail.* 2011;13(1):18–28. [PubMed: 20685685]
22. Ferrari R, Böhm M, Cleland JG, et al. Heart failure with preserved ejection fraction: uncertainties and dilemmas. *Eur. J. Heart Fail.* 2015;17(7):665–71. [PubMed: 26079097]
23. Schiattarella GG, Sequeira V, Ameri P. Distinctive patterns of inflammation across the heart failure syndrome. *Heart Fail. Rev.* 2020;1–12. [PubMed: 31414215]
24. Kawano H, Motoyama T, Hirashima O, et al. Hyperglycemia rapidly suppresses flow-mediated endothelium-dependent vasodilation of brachial artery. *J. Am. Coll. Cardiol.* 1999;34(1):146–54. [PubMed: 10400004]
25. Ahmad A, Corban MT, Toya T, et al. Coronary microvascular dysfunction is associated with exertional haemodynamic abnormalities in patients with heart failure with preserved ejection fraction. *Eur. J. Heart Fail.* 2021;23(5):765–72. [PubMed: 32949186]
26. Schiattarella GG, Altamirano F, Tong D, et al. Nitrosative stress drives heart failure with preserved ejection fraction. *Nature.* 2019;568(7752):351–6. [PubMed: 30971818]
27. Chirinos JA, Zamani P. The nitrate-nitrite-NO pathway and its implications for heart failure and preserved ejection fraction. *Curr. Heart Fail. Rep.* 2016;13(1):47–59. [PubMed: 26792295]
28. Moraes RdA, Webb RC, Silva DF. Vascular Dysfunction in Diabetes and Obesity: Focus on TRP Channels. *Front. Physiol.* 2021;12:225.
29. Hwang SW, Cho H, Kwak J, et al. Direct activation of capsaicin receptors by products of lipoxygenases: endogenous capsaicin-like substances. *Proc. Natl. Acad. Sci. U. S. A.* 2000;97(11):6155–60. [PubMed: 10823958]
30. Kolijn D, Pabel S, Tian Y, et al. Empagliflozin improves endothelial and cardiomyocyte function in human heart failure with preserved ejection fraction via reduced pro-inflammatory-oxidative pathways and protein kinase G $\alpha$  oxidation. *Cardiovasc. Res.* 2021;117(2):495–507. [PubMed: 32396609]
31. Mori J, Patel VB, Abo Alrob O, et al. Angiotensin 1–7 ameliorates diabetic cardiomyopathy and diastolic dysfunction in db/db mice by reducing lipotoxicity and inflammation. *Circ. Heart Fail.* 2014;7(2):327–39. [PubMed: 24389129]
32. Guimbal S, Cornuault L, Hollier P-L, et al. Mast cells participate in the development of diastolic dysfunction in diabetic obese mice. *bioRxiv.* 2020.
33. Toth A, Czikora A, Pasztor ET, et al. Vanilloid receptor-1 (TRPV1) expression and function in the vasculature of the rat. *J. Histochem. Cytochem.* 2014;62(2):129–44. doi:10.1369/0022155413513589 [PubMed: 24217926]
34. Zhao F, Fu L, Yang W, et al. Cardioprotective effects of baicalein on heart failure via modulation of Ca $^{2+}$  handling proteins in vivo and in vitro. *Life Sci.* 2016;145:213–23. [PubMed: 26706290]
35. Baral P, Udit S, Chiu IM. Pain and immunity: implications for host defence. *Nature Reviews Immunology.* 2019;19(7):433–47.

36. Hulsmans M, Sager HB, Roh JD, et al. Cardiac macrophages promote diastolic dysfunction. *J. Exp. Med.* 2018;215(2):423–40. [PubMed: 29339450]

Author Manuscript

Author Manuscript

Author Manuscript

Author Manuscript

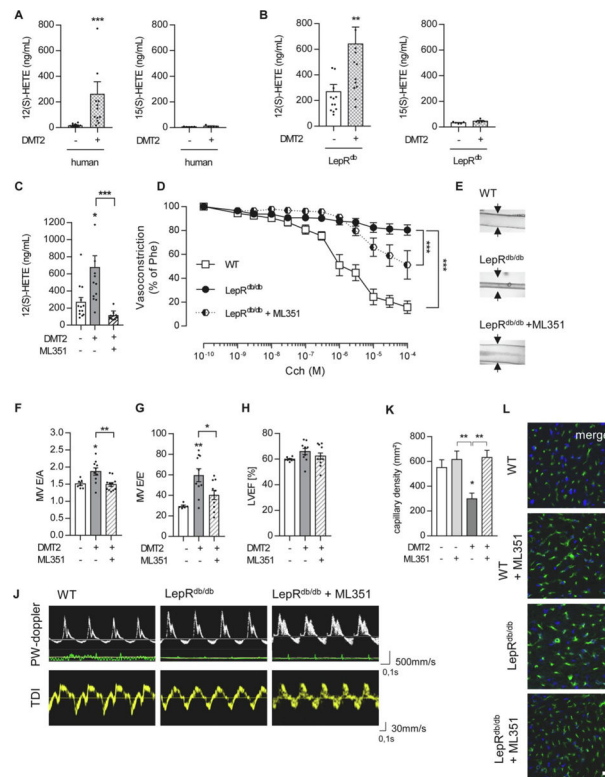


**Figure 1. Reduction of 12(S)-HETE levels ameliorates vascular function and mitigates HFpEF in type 2 diabetic mice.**

12(S)-HETE and 15(S)-HETE plasma levels in (A) human diabetic patients, n=13 patients/group, (B) 12-week old non-diabetic, *LepR<sup>db/+</sup>* and diabetic, *LepR<sup>db/db</sup>* mice, n=13 mice/group, \*\*P<0.01, \*\*\*P<0.001 vs. control, Mann-Whitney U-test. (C) Murine 12(S)-12LOX inhibitor ML351 for 7 consecutive days. n=10–14 mice/group, Kruskal-Wallis test, \*P<0.05, \*\*\*P<0.001, vs. controls or as indicated. (D) Carbamoylcholine (Cch) induced vasorelaxation in murine mesenteric resistance arteries precontracted with  $10^{-5}$ M phenylephrine (Phe) was impaired in diabetic *LepR<sup>db/db</sup>* mice (black circle) compared to non-diabetic *LepR<sup>db/+</sup>* mice (white square). ML351 treatment (circle half black) improved vascular function compared to control-treated mice. n=8–12 mice/group, Two-way ANOVA/Bonferroni, \*\*\*P<0.001 as indicated. (E) Pictures show representative murine resistance arteries and their response to Cch-induced vasorelaxation at  $10^{-5}$ M. (F) Ratio between early-to-late stage (E/A) diastolic filling, (G) mitral wave E to E' wave (E/E') ratio and (H) left ventricular ejection fraction (LVEF) of *LepR<sup>db/+</sup>*, *LepR<sup>db/db</sup>* with or without 7 days of intraperitoneal ML351 injections. n=6–12 mice/group, One-way ANOVA/Bonferroni, \*P<0.05, \*\*P<0.001 vs. control or as indicated. (J) Representative pulsed-wave Doppler (PW-doppler, top) and tissue doppler imaging (TDI, bottom) tracings. (K) Quantification of capillary density in murine left ventricular muscle tissue, n=5 mice/group, Kruskal-Wallis test, \*P<0.05, \*\*P<0.01 vs. control or as indicated. (L) Immunohistochemistry of murine, frozen heart sections showing CD31-positive (green) areas representing capillaries, and cell nuclei stained with DAPI (blue). Reduced capillary density in *LepR<sup>db/db</sup>* vs. *LepR<sup>db/+</sup>* was ameliorated in *LepR<sup>db/+</sup>* with ML351 injections. Scale bars indicate 10 $\mu$ m. All graphs show mean $\pm$ SEM. DMT2 – type 2 diabetes mellitus, WT-wild type.



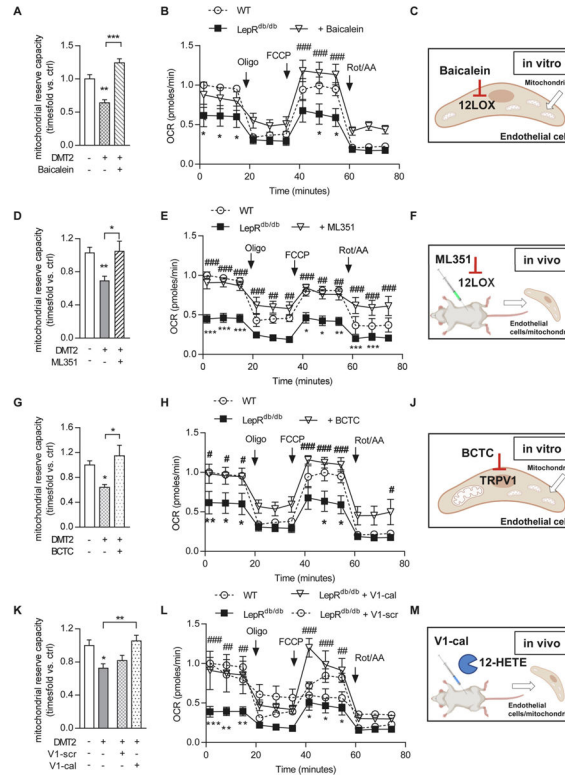


**Figure 2. Mitochondrial function is improved in endothelial cells from type 2 diabetic mice by interfering with 12(S)-HETE/TRPV1 interaction.**

Mitochondrial reserve capacity (A, K, One-way ANOVA/Bonferroni, D, G Kruskal-Wallis test) and mitochondrial oxygen consumption rate (OCR, B, E, H, L, Two-way ANOVA/Bonferroni) in endothelial cells isolated from diabetic vs. non-diabetic mice, 5–8 mice/group. Maximum mitochondrial respiration was assessed after addition of oligomycin (Oligo) and FCCP indicated by arrows. Mitochondrial reserve capacity calculated by subtracting basal mitochondrial OCR from maximum OCR. Data is presented as mean±SEM, \*P<0.05, \*\*P<0.01, \*\*\*P<0.001 WT vs. LepR<sup>db/db</sup> and #P<0.05, ##P<0.01, ###P<0.001 LepR<sup>db/db</sup>+treatment vs. LepR<sup>db/db</sup>. Illustrations indicate the application of the 12/15LO inhibitor baicalein to isolated endothelial cells in vitro (C), i.p. application in vivo of the 12/15LO inhibitor ML351 with consecutive endothelial cell isolation for mitochondrial functional analysis in vitro (F), the TRPV1 inhibitor BCTC to isolated endothelial cells in vitro (J) and the intravenous application of the V1-cal or V1-scr peptide in vivo with consecutive endothelial cell isolation for mitochondrial functional analysis in vitro (M). WT-wild type, Rot/AA – rotenone/antimycin A.

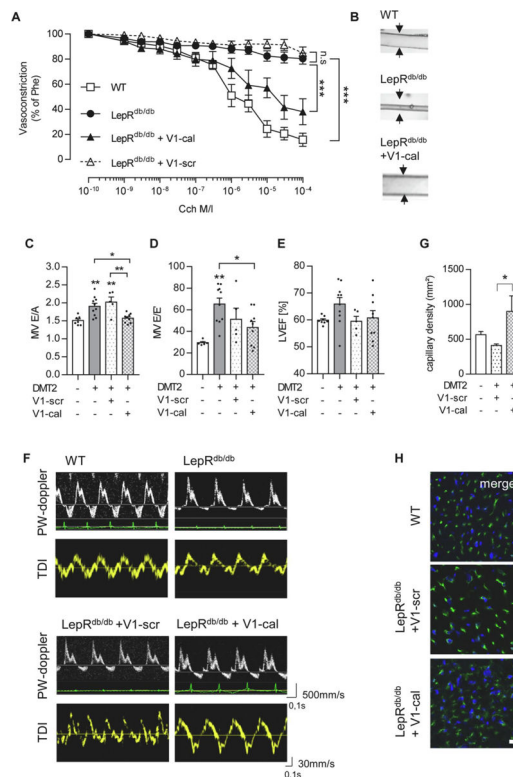


**Figure 3. Inhibiting 12(S)-HETE/TRPV1 interaction improves vascular dysfunction and diminishes HFpEF manifestation.**

(A) Carbamoylcholine (Cch) induced vasoconstriction in murine mesenteric resistance arteries precontracted with  $10^{-5}$ M phenylephrine (Phe) was improved in diabetic LepR<sup>db/db</sup> after intravenous injections for 4 consecutive days of the V1-cal peptide, but not V1-scr, a scrambled version of V1-cal, compared to control mice.  $n=8-12$  mice/group, Two-way ANOVA/Bonferroni, \*\*\* $P<0.001$  as indicated, n.s. not significant. (B) Pictures show representative murine resistance arteries and their response to Cch-induced vasoconstriction at  $10^{-5}$ M after precontraction. Intravenous injection of V1-cal but not V1-scr improved (C) ratio between early-to-late stage (E/A) diastolic filling, (D) mitral wave E to E' wave (E/E') ratio and (E) left ventricular ejection fraction (LVEF) of LepR<sup>db/db</sup> vs. LepR<sup>db/+</sup>.  $n=6-10$  mice/group, One-way ANOVA/Bonferroni, \* $P<0.05$ , \*\* $P<0.01$  control or as indicated. (F) Representative pulsed-wave Doppler (PW-doppler, top) and tissue doppler imaging (TDI, bottom) tracings for data quantified in C-E. (G) V1-cal but not V1-scr increased capillary density in left ventricular cardiac tissue. Graph shows quantification of images in H for capillary density per mm<sup>2</sup> in LepR<sup>db/+</sup> vs. LepR<sup>db/db</sup> with V1-scr or V1-cal treatment. 2 randomized areas were analysed per mouse by a blinded observer,  $n=4-5$  mice/group, One-way ANOVA/Bonferroni, \* $P<0.05$  as indicated. (H) CD31 immunofluorescence staining of murine heart sections showing CD31-positive (green) capillaries and DAPI-stained cell nuclei (blue). Scale bar indicates 10 $\mu$ m. All graphs show mean $\pm$ SEM. DMT2 – type 2 diabetes mellitus, WT-wild type.

**Table 1:**

Clinical and laboratory parameters of diabetic vs. non-diabetic patients.

	<b>Non-Diabetic</b>	<b>Diabetic</b>	
	<b>n=13</b>	<b>n=13</b>	<b>P value</b>
Age (years)	65.4 ± 6	68.2 ± 6	0.24
Male n (%)	7 (46)	12 (92)	0.08
Body mass index (kg/m <sup>2</sup> )	n.d.	30.7 ± 4.9	n.d.
Fasting glucose (mg/dL)	n.d.	139 ± 39	n.d.
HbA1c (%)	5.6 ± 0.3	7.2 ± 0.9	<b>&lt;0.001</b>
Oral anti-diabetics n (%)	0 (0)	13 (100)	<b>&lt;0.001</b>
Insulin treatment n (%)	0 (0)	13 (100)	<b>&lt;0.001</b>
Arterial hypertension n (%)	2 (15)	13 (100)	0.157
Anti-hypertensive medication n (%)	3 (23)	13 (100)	0.08
Reported diastolic dysfunction n (%)	0 (0)	13 (100)	<b>&lt;0.001</b>
12(S)-HETE (ng/mL)	17.6 ± 10	264.2 ± 336	<b>0.014</b>

Values are presented as mean±SD or n in % of total cohort. P-values were determined by Student's t-test, except for Type 2 diabetes mellitus (DM), medication and hypertension (categorical variables). Bold P-values indicate significance, n.d. - not determined.